

Interaction of silicene and germanene with non-metallic substrates

M Houssa¹, E Scalise², B van den Broek¹, A Lu^{1,3}, G Pourtois³, V V Afanas'ev¹, and A Stesmans¹

¹ Department of Physics and Astronomy, University of Leuven, B-3001 Leuven, Belgium

² Max Planck Institut für Eisenforschung, 40237 Düsseldorf, Germany

³ imec, 75 Kapeldreef, B-3001 Leuven, Belgium

Abstract. By using first-principles simulations, we investigate the interaction of silicene and germanene with various non-metallic substrates. We first consider weak van der Waals interactions between the 2D layers and dichalcogenide substrates, like MoX₂ (X=S, Se, Te). The buckling of the silicene or germanene layer is correlated to the lattice mismatch between the 2D material and the MoX₂ template. The electronic properties of silicene or germanene on these different templates then largely depend on the buckling of the 2D material layer: highly buckled silicene or germanene on MoS₂ are predicted to be metallic, while low buckled silicene on MoTe₂ is predicted to be semi-metallic, with preserved Dirac cones at the K points. We next study the covalent bonding of silicene and germanene on (0001) ZnS and ZnSe surfaces. On these substrates, silicene or germanene are found to be semiconducting. Remarkably, the nature and magnitude of their energy band gap can be controlled by an out-of-plane electric field.

1. Introduction

Very recently, the formation of silicene, the silicon counterpart of graphene, was reported on (111)Ag surfaces [1-3], as well as on (0001)ZrB₂ [4] and (111)Ir [5] surfaces. The electronic properties of the silicene layer on (111)Ag was investigated using angle-resolved photoemission spectroscopy. These measurements revealed the presence of a linear dispersion in the band structure of silicene (so called Dirac cones) with a Fermi velocity of about 1.3×10^6 m/s [3], as theoretically predicted for free-standing silicene [6].

The possible existence of silicene was so far reported on these metallic substrates. However, the characterization of the electronic and electrical properties of silicene and germanene on metallic substrates is very challenging, since these properties are then largely dominated by the metal. The growth of silicene and germanene on semiconducting or insulating substrates is required for their firm identification and complete characterization. In addition, potential applications of these 2D materials in nanoelectronic devices will also require their growth on non-metallic substrates.

We first theoretically study the weak (van der Waals) interaction of silicene and germanene with layered dichalcogenide substrates [7]. On these templates, silicene and germanene are predicted to be either metallic or semi-metallic (with preserved Dirac cones at the k-points), depending on the buckling of the 2D layer.

We next investigate the covalent bonding of silicene and germanene on (0001)ZnS and ZnSe surfaces [8,9]. The charge transfer occurring at the silicene/(0001) ZnS and germanene/(0001) ZnSe



interface leads to the opening of an indirect energy band gap in silicene or germanene. Very interestingly, it is found that the nature (indirect or direct) and magnitude of their energy band gap can be controlled by an external electric field.

2. Theoretical details

First-principles simulations were performed using density functional theory (DFT). The generalized gradient approximation (GGA) was used for the exchange-correlation functional [10], as implemented in the Siesta package [11] or in the plane-wave Quantum Espresso package [12]. The core electrons were implicitly treated by using norm-conserving pseudopotentials [13] and the valence electrons were described by using double zeta singly polarized basis sets (Siesta) or plane-wave basis sets (Quantum Espresso). An energy cutoff of 300 Ry and a (10x10x1) k-point mesh were used for the computations, allowing convergence of the total energy of the systems below typically 10 meV. The atomic structure optimization was carried out by relaxing the forces on all atoms until a 0.05 eV/Å force tolerance was reached, using a conjugate gradient method. The computations were performed on periodic slab models, with about 15 Å of vacuum between the periodic cells, in order to minimize the interaction between neighboring cells. To study the effect of an external electric field on the electronic properties of the silicene/(0001) ZnS and silicene/(0001) ZnSe interfaces, a periodic zigzag electric potential was applied in the direction perpendicular to the interface.

3. Silicene and germanene on MoX₂ substrates

We first considered the interaction of silicene and germanene with different semiconducting dichalcogenide substrates, namely MoX₂ with X=S, Se, Te [7]. The computed in-plane lattice parameters and energy band gap of these substrates are given in Table 1.

Table 1. Computed in-plane lattice parameters and energy band gaps of MoX₂.

	In-plane lattice parameter (Å)	Energy band gap (eV)
MoS ₂	3.16	1.2
MoSe ₂	3.30	1.1
MoTe ₂	3.52	1.0

The initial atomic configuration consists in a supercell with a flat silicene or germanene layer on top of “bulk” MoX₂ (which includes 4 atomic layers). The two bottom MoX₂ layers were kept fixed during relaxation and the initial distance between the 2D material and the top MoX₂ layer equals 4.5 Å. The cell parameter was kept to the one of the template, the silicene or germanene layer being compressively strained, as compared to the free-standing case. We studied three different possible arrangements of the silicon or germanium atoms with respect to the underlying Mo and X atoms, as shown Fig.1: (a) Si (Ge) hexagons placed on top of the MoX₂ hexagons – so called AAA stacking like in h-BN, (b) Si (Ge) hexagons shifted with respect to the MoX₂ hexagons by half a unit cell, and (c) Bernal-like arrangement (ABA stacking), like in graphite.

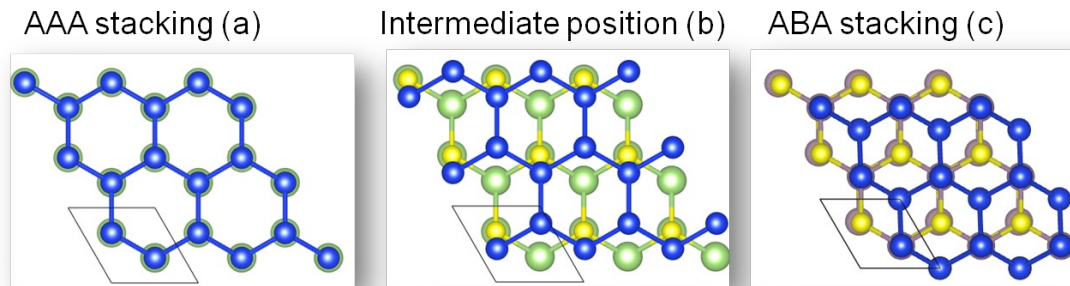


Figure 1. Three different atomic arrangements of the silicene layer on top of MoS₂. Blue, yellow and green spheres are Si, S and Mo atoms, respectively.

After energy relaxation, (a) and (c) structures kept their initial configuration, while structure (b) relaxed to configuration (c). The energy difference between the various configurations is typically less than 5 meV/atom, these atomic configurations being thus equally stable (degenerate). This indicates that the interaction between silicene or germanene layer with the dichalcogenide substrate is very weak. On the other hand, the difference in energy between the initial (before relaxation) and the final (after relaxation) structures is more than 0.1 eV/atom. This energy difference is mainly due to the buckling of the silicene or germanene layer. In all the three structures, the 2D material indeed buckled after relaxation; the buckling distance is given in Table 1 for the silicene/MoX₂ system, together with the in-plane lattice parameter mismatch. From these results, the buckling distance is clearly correlated to the in-plane lattice mismatch. Note that the typical silicene-MoX₂ interlayer distance lies between 3 and 3.5 Å.

Table 2. Silicene buckling distance and in-plane lattice mismatch between silicene and the dichalcogenide substrate.

	Buckling distance (Å)	In-plane lattice mismatch (%)
MoS ₂	1.9	18
MoSe ₂	1.0	14
MoTe ₂	0.7	9

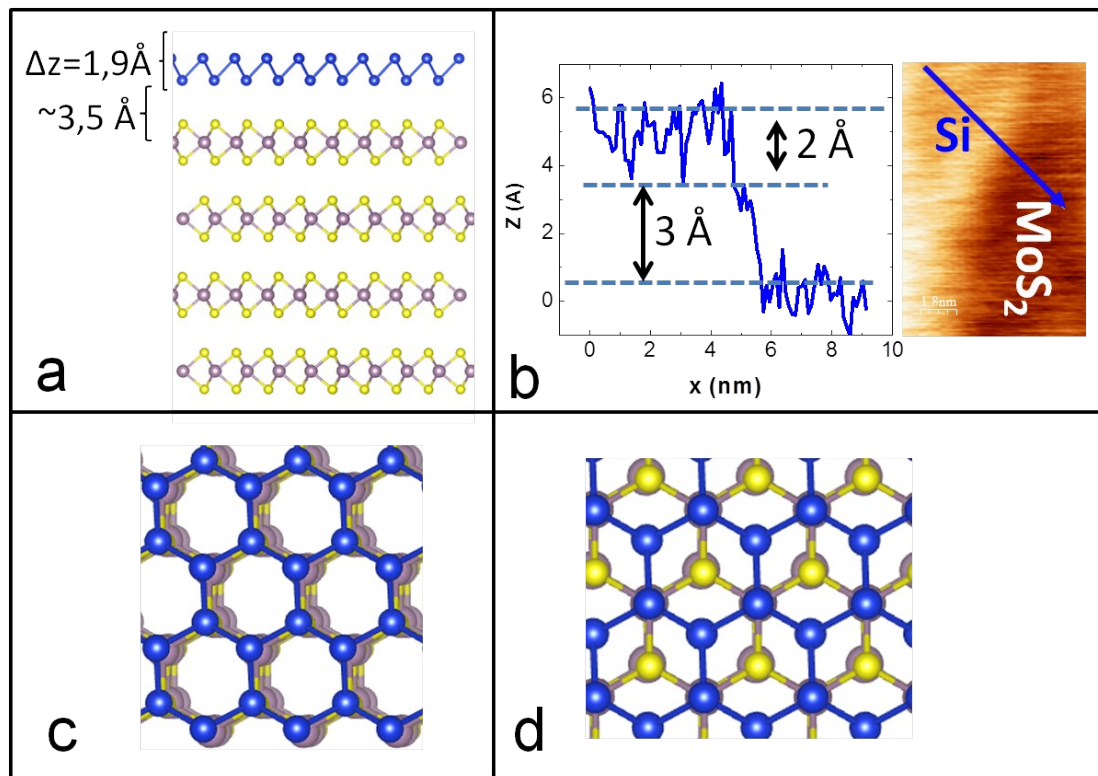


Figure 2. (a) Relaxed atomic configuration of silicene on bulk MoS_2 (side view). In (b) the STM image ($V_B=0.2\text{V}$, $I_S=2\text{nA}$) of a partially covered MoS_2 surface by Si atoms is shown (right side). A line profile taken across the two terraces allows measuring the amplitude of the step which amounts to about 5 \AA (left side of b). In (c) and (d), the top view of *a* and *c* configurations from Fig. 1 (obtained after atomic relaxation) are shown. Blue, yellow and green spheres are Si, S and Mo atoms, respectively. The experimental results are from ref. 14.

Both the Si buckling distance and the Si- MoS_2 interlayer distance are in very good agreement with recently reported experimental STM results [14], see Fig. 2.b, where the step profile between a Si domain and the MoS_2 substrate amounts to 3 \AA and exhibits a feature at about 2 \AA , consistently with the highly buckled silicene arrangement (see the picture in Fig. 2.a). The relatively good agreement between the experimental and computed structural properties of silicene on MoS_2 is supporting the validity of our theoretical approach.

The predicted electronic structure of the silicene and germanene layer on the MoX_2 template largely depends on the buckling parameter in the 2D material. Highly buckled silicene or germanene are predicted to be metallic, as illustrated in Fig. 3 for the case of silicene on MoS_2 . On the other hand, the low buckled silicene layer on MoTe_2 is predicted to preserve its Dirac cones at the K points, as illustrated in Fig. 4. Silicene on MoTe_2 is thus predicted to be a gapless semiconductor, similar to free standing silicene. By increasing the in-plane lattice parameter of the dichalcogenide substrates, we thus found out that the buckling distance in the silicene or germanene layer can be reduced and the 2D material can eventually preserve its gapless semiconducting behavior, i.e. the partial sp^2 hybridization of the Si and Ge atoms is preserved.

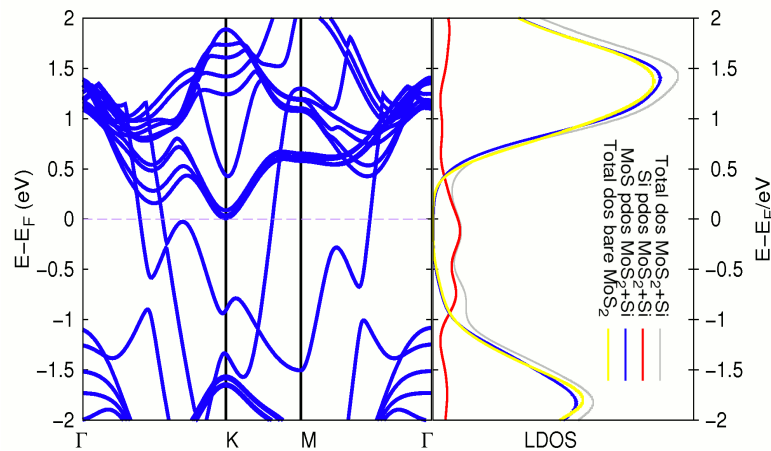


Figure 3. Energy band structure and local density of states (LDOS) of the silicene/MoS₂ structure. The LDOS shows that the density of states of the MoS₂ substrate still preserve a gap very close to that of the bare MoS₂, while all the electronic states close to the Fermi level are due to the contribution of Si atoms, confirming that almost no “interaction” (e.g. hybridization) between Si and Mo/S atomic orbitals is induced.

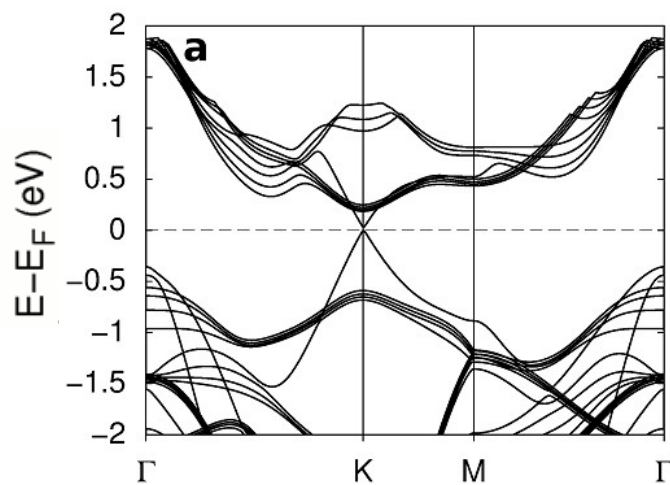


Figure 4. Energy band structure of the silicene/MoTe₂ system.

4. Silicene/ZnS and germanene/ZnSe interfaces

ZnS and ZnSe are semiconductors with a large direct energy band-gap of about 3.8 eV and 2.9 eV, respectively [15,16]. Very interestingly, the in-plane lattice constants of ZnS (3.81 Å) and ZnSe (3.98 Å) are very close to the computed ones of free-standing silicene and germanene, i.e. about 3.9 Å and 4.0 Å, respectively; ZnS and ZnSe thus appear as semiconducting templates with adequate symmetry and in-plane lattice parameters for the growth of silicene and germanene, respectively. Since the structural and electronic properties of the silicene/(0001) ZnS and germanene/(0001)ZnSe structures

are qualitatively very similar, we only discuss here in details the results pertaining to the germanene/ZnSe interface; results about the silicene/(0001) ZnS interface can be found elsewhere [8].

We first computed the lattice parameters of bulk (wurtzite) ZnSe, which were found to be $a=b=3.94$ Å and $c=6.54$ Å, typically 1% smaller than the experimental values. The calculated energy gap is 2.4 eV, i.e. about 17% smaller than its experimental value. We next constructed (0001) polar ZnSe surfaces. A slab model with 8 atomic layers was considered (with a total of 64 atoms), with a 15 Å vacuum layers. After energy relaxation, the atoms of the top and bottom ZnSe layers are displaced, leading to a surface reconstruction very similar to the one of the non-polar (1010) ZnS surface [17,18]; this surface reconstruction is discussed in detail elsewhere [8]. A very similar surface reconstruction was reported recently on (0001) ZnS surfaces, and predicted to be more stable than the non-reconstructed polar ZnS surface for layers up to about 6.6 nm [19]. The reconstructed (0001) ZnSe surface is semiconducting, with a computed energy gap of about 2.1 eV. Note that polar (non-reconstructed) ZnS and ZnSe surfaces are metallic, due to the pinning of the Fermi level by the anion surface states, like in ZnO [20,21]. On such polar surfaces, both silicene and germanene were also found to present a metallic character [22].

We next investigated the interaction of germanene with the reconstructed (0001) ZnSe surface. A flat germanene layer was placed on top of the reconstructed (0001) ZnSe surface, followed by geometry relaxation. As discussed in more details in ref. 8 for the case of silicene on ZnS, we studied different possible arrangements of the Ge atoms on the (0001) ZnSe surface. The most energetically stable structure corresponds to an hexagonal arrangements of the Ge atoms placed at intermediate positions between top and hollow sites of the ZnSe hexagons, as shown in Fig. 5. In this geometry, 2 Ge-Se (2.58 Å bond length) and 2 Ge-Zn bonds (2.49 Å bond length) are formed; the electronic charge transfer essentially occurs between the $4p_z$ orbitals of the Ge atoms with the $4s$ states of Zn and $4p$ states of Se, the bonded Ge atoms thus adopting an sp^3 -like character. Four other Ge atoms from the silicene layer are not bonded to the substrate: two of these atoms are lying at about 2.9 Å from the ZnSe surface, and are marked "intermediate" on Fig. 5 and two other atoms are lying at about 3.71 Å from the ZnSe surface, and are marked "top" on Fig. 5. From the analysis of the partial Mulliken charges on the Ge atoms, the charge transfer occurring at the germanene/(0001) ZnSe interface leads to an excess of negative charge of about 0.15 e on the top Ge atoms, with respect to the intermediate Ge atoms, thus leading to the formation of a dipole at this interface. The average Ge-Ge distance is calculated to be 2.49 Å, very similar to the one of free-standing germanene.

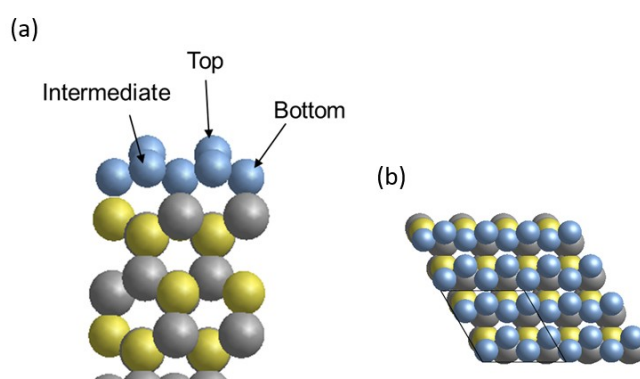


Figure 5. Side view (a) and top view (b) of the relaxed germanene/(0001) ZnSe slab model. Yellow, gray and blue spheres are Se, Zn and Ge atoms, respectively.

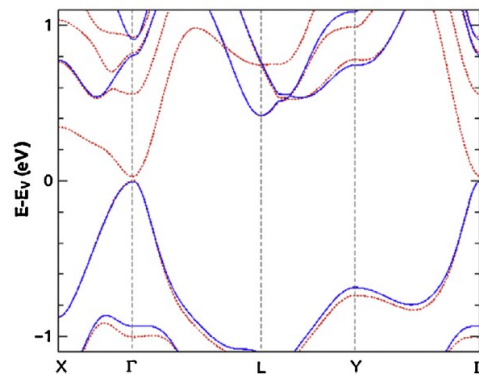


Figure 6. Computed energy band structure of the germanene/(0001) ZnSe slab model, without (solid blue lines) and with (dashed red lines) an external electric field of $0.6 \text{ V}/\text{\AA}$ in the direction perpendicular to the interface. The reference (zero) energy level corresponds to the top of the valence band E_v of germanene.

The computed energy band structure of the germanene/(0001)ZnSe slab model is shown in Fig. 6. The system is predicted to be semiconducting, with an indirect energy band gap of about 0.4 eV . The opening of an energy gap in the electronic structure of germanene is related to the charge transfer and partial sp^3 hybridization of the Ge atoms bonded to the Zn or Se atoms on the surface. As a matter of fact, the computation of the electronic DOS of a germanene layer with the same atomic arrangement than observed on the ZnSe surface, but with the ZnSe substrate removed, presents a gapless-semiconducting behaviour (not shown).

We next studied the effect of an external electric field on the electronic properties of the germanene/(0001) ZnSe interface. The energy band structure of the system is shown in Fig. 6, without (solid lines) and with (dashed lines) an external electric-field of $0.6 \text{ V}/\text{\AA}$. Very interestingly, the applied electric field has a substantial effect on the conduction band near the Γ point, leading to a transition from an indirect (Γ to L point) to direct (at Γ point) energy band gap in germanene. The computed direct and indirect energy band gaps are shown in Fig. 7 as a function of the external electric field. For electric fields lower than about $0.4 \text{ V}/\text{\AA}$, the germanene/(0001) ZnSe interface has an indirect energy band gap, which is almost unaffected by the external electric field. For larger electric fields, the energy band gap becomes direct, and its value decreases approximately linearly with the external electric field, a semiconductor to metal transition being predicted for electric fields higher than $0.6 \text{ V}/\text{\AA}$. The electric field dependence of the energy gap of germanene/(0001)ZnSe is very similar to the one of the silicene/(0001) ZnS system, which has been discussed in more detail elsewhere [8]; it is related to the reduced dipole at the silicene/ZnS interface in presence of an external electric field.

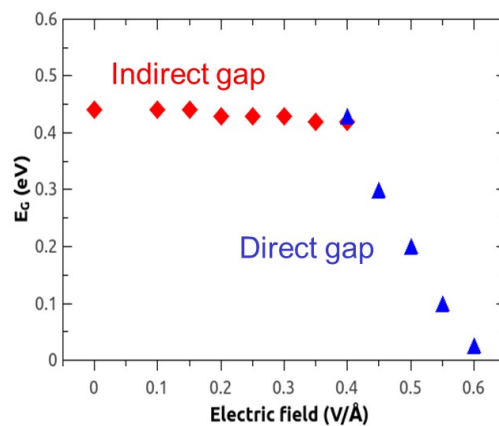


Figure 7. Computed direct (filled triangles) and indirect (filled diamonds) energy band gaps of the germanene/(0001) ZnSe slab model, as a function of the external electric field applied to the system.

5. Conclusions

The interaction of silicene and germanene with several non-metallic substrates has been theoretically investigated. On dichalcogenides, the 2D material is weakly bonded to the substrate, via van der Waals forces. The buckling distance in silicene or germanene is correlated to the lattice parameter of the dichalcogenide template. On MoS_2 , silicene and germanene are highly buckled, and are metallic. On MoTe_2 , silicene is weakly buckled and its (partial) sp^2 hybridization is preserved, the material being a gapless semiconductor. Our theoretical findings thus suggest that the electronic properties of silicene and germanene can be engineered by properly tuning the in-plane crystal parameters “matching” between the 2D material and the dichalcogenide substrate. These non-metallic compounds thus appear as potential templates for the growth of silicene and germanene, potentially enabling their use in future nanoelectronic devices.

On reconstructed (0001) ZnS and ZnSe surfaces, the silicene and germanene layers adopt the surface reconstruction of the underlying ZnS or ZnSe layer, and part of the Si (Ge) atoms are forming bonds with Zn or S (Se) atoms. The bonded Si (Ge) atoms present a sp^3 -like hybridization, leading to the formation of silicene (germanene) with an indirect energy band-gap. Remarkably, the value and nature (direct or indirect) of the energy gap of the silicene/(0001) ZnS and germanene/(0001) ZnSe interfaces can be controlled by an external electric field. This predicted electric-field modulation of the electronic properties of silicene and germanene is potentially very interesting for logic applications.

Acknowledgements

Part of this work has been financially supported by the European Project 2D-NANOLATTICES, within the Future and Emerging Technologies (FET) program of the European Commission, under the FET-grant number 270749 as well as the Research Fund of KU Leuven, project GOA/13/011.

References

- [1] Vogt P, De Padova P, Quaresima C, Avila J, Frantzeskakis E, Asensio M C, Resta A, Ealet B and Le Lay G 2012 *Phys. Rev. Lett.* **108** 155501
- [2] Feng B, Ding Z, Meng S, Yao Y, He X, Cheng P, Chen L and Wu K 2012 *Nano Lett.* **12** 3507
- [3] Chiappe D, Grazianetti C, Tallarida G, Fanciulli M and Molle A 2012 *Adv. Mat.* **24** 5088
- [4] Fleurence A, Friedlein R, Ozaki T, Kawai H, Wang Y and Yamada-Takamura Y 2012 *Phys. Rev. Lett.* **108** 245501
- [5] Meng L, Wang Y, Zhang L, Du S, Wu R, Li L, Zhang Y, Li G, Zhou H, Hofer W A and Gao M J 2013 *Nano Lett.* **13** 685
- [6] Houssa M, Pourtois G, Heyns M M, Afanas'ev V V and Stesmans A 2011 *J. Electrochem. Soc.* **158** H107
- [7] Scalise E, Houssa M, Cinquanta E, Grazianetti C, van den Broek B, Pourtois G, Stesmans A, Fanciulli M and Molle A 2014 *2D Mater.* **1** 011010
- [8] Houssa M, van den Broek B, Scalise E, Pourtois G, Afanas'ev V V and Stesmans A 2013 *Phys. Chem. Chem. Phys.* **15** 3702
- [9] Houssa M, van den Broek B, Scalise E, Ealet B, Pourtois G, Chiappe D, Cinquanta E, Grazianetti C, Fanciulli M, Molle A, Afanas'ev V V and Stesmans A 2014 *Appl. Surf. Sci.* **291** 98
- [10] Perdew J, Burke K and Ernzerhof M 1996 *Phys. Rev. Lett.* **77** 3865
- [11] Soler J M, Artacho E, Gale J D, García A, Junquera J, Ordejón P and Sánchez-Portal D 2002 *J. Phys. C: Cond. Matter* **14** 2745
- [12] Giannozzi P *et al.* 2009 *J. Phys.: Cond. Matter* **21** 395502
- [13] Troullier N and Martins J L 1991 *Phys. Rev. B* **43** 1993
- [14] Chiappe D, Scalise E, Cinquanta E, Grazianetti C, van den Broek B, Fanciulli M, Houssa M and Molle A 2014 *Adv. Mat.* **26** 2096
- [15] Weber M J 1986 *Handbook of Laser Science and Technology* (Cleveland: CRC Press)
- [16] Xu Y N and Ching W Y 1993 *Phys. Rev. B* **48** 4335
- [17] Northrup J E and Neugebauer J 1996 *Phys. Rev. B* **53** R10477
- [18] Filippetti A, Fiorentini V, Cappellini G and Bosin A 1999 *Phys. Rev. B* **59** 8026
- [19] Zhang X, Zhang H, He T and Zhao M 2010 *J. Appl. Phys.* **108** 064317
- [20] Wander A, Schedin F, Steadman P, Norris A, McGrath R, Turner T S, Thornton G and Harrison N M 2001 *Phys. Rev. Lett.* **86** 3811
- [21] Meyer B and Marx D 2003 *Phys. Rev. B* **67** 035403
- [22] Houssa M, van den Broek B, Scalise E, Pourtois G, Afanas'ev V V and Stesmans A 2013 *ECS Trans.* **53** 51